AL-Bahir
Journal for Engineering and Pure Sciences
BJEPS

Volume 3 | Issue 2 Article 4

Concentration of Spraying Solution Effect on the Structural, Morphological and Optical Properties of NiO Thin Films

Radhiyah M. Aljarrah
University of Kufa/ Faculty of Science/ Department of Physics/ Najaf, Iraq

Ali Madlool Naamah
University of Babylon/ Faculty of Science/ Department of Physics / Babylon, Iraq

Adel H. Omran Alkhayatt
University of Kufa/ Faculty of Science/ Department of Physics/ Najaf, Iraq

ORIGINAL STUDY

Concentration of Spraying Solution Effect on the Structural, Morphological and Optical Properties of NiO Thin Films

Radhiyah M. Aljarrah [a], Ali Madlool Naamah [b], Adel H. Omran Alkhayatt [a,*]

[a] University of Kufa, Faculty of Science, Department of Physics, Najaf, Iraq
[b] University of Babylon, Faculty of Science, Department of Physics, Babylon, Iraq

Abstract

In the present study nickel oxide NiO thin films of thickness ranging about 250−350 nm which were prepared on glass substrates by using chemical spray pyrolysis as a simple and low cost method. The impact of thickness and aqueous solution molarity concentration on the crystal structure and optical characteristics were investigated. The results showed that the deposited films is homogenous and have a good adherent to the glass substrates. The crystal structure results showed that all films have polycrystalline in nature, of rock salt phase, and the preferential orientation is an along (111) plane. The diffraction intensity was increased with the increase in spray solution concentration, leading to the enhancement of the crystallinity and an increase in the crystallite size from 9.7 nm to 28.5 nm and reducing the dislocation density from (104.3−12.2) × 10^{16} line/m^2. While the results of AFM results show that the grain size (D) enlarges with increasing molarities concentration. Transmittance spectra confirm that the optical transmittance is of the direct allowed type, while the value of transparency ranged from moderate to weak value and decrease when the spray solution molar concentration and film thickness increases. Whereas the forbidden energy gap was decremented with the increment of molarity concentration of spray solution and film thickness from 3.85 to 3.15 eV.

Keywords: Absorbance, Energy gap, Rock salt, Spray pyrolysis, Transmittance

1. Introduction

Nanomaterials emerged as a fantastic class of materials that own a wide spectrum of examples with one or more dimensions in the range of 1−100 nm. The new features that appear in the case of the materials are due to the appearance of the boundary effect of the particles that are constituents of the nanomaterial [1]. The exceptionally high ratio of surface area to volume of the nanoparticle can be achieved by controlling the buildup of the nanoparticles. Nanomaterials have been produced with magnetic, electrical, optical, mechanical, and catalytic properties that are completely different from their bulk form. The nanostructure form of semiconductor materials is a leading type of material, giving wide freedom to determine electronic and optoelectronic properties which makes them more suitable for photocatalytic, photo voltaic applications [2]. Over the past decades and so far, most of the researchers and demanders had focused on the wide optical gap semiconductor and transparent conducting oxides TCO materials. Due to its high transmittance in the Vis region, high conductivity, and high reflectance in the IR region. Such as SnO_2 of 3.6 eV direct band gap and n-type conductivity [3], CuO of 2.1 eV direct band gap, and p-type conductivity [4], ZnO of 3.37 eV direct band gap and n-type conductivity [5], and NiO of 3.5 eV direct band gap and p-type semiconductor [6]. These materials are preferred due to their stability, chemical inertness, resistance the high temperature, and mechanical hardness [7−10]. Nickel oxide (NiO) is a metal oxide that has been studied extensively due to

Received 22 May 2023; revised 19 July 2023; accepted 19 July 2023.
Available online 02 September 2023

* Corresponding author.
E-mail addresses: radhiyah.aljarrah@uokufa.edu.iq (R.M. Aljarrah), adilh.alkhayat@uokufa.edu.iq (A.H. Omran Alkhayatt).

https://doi.org/10.55810/2313-0083.1039

its many desirable properties, including its low cost, wide availability, photo-stability, non-toxicity, and various catalytic activities [11,12]. Nickel oxide physically is a greenish gray powder depending on the kind of preparation method, made up of nickel and oxygen, therefore it is classified as II–VI composite semiconductor, with a face center cubic structure and it has many applications [13]. NiO is a P-type semiconductor, which owns direct band gaps of 3.5–3.8 eV, and weakly absorption band in the visible range [14–17]. At room temperature nickel oxide is an insulator; however at high temperatures the structural defect makes it a semiconductor [18]. Nickel oxide thin films can be prepared by various methods which include: magnetron sputtering [19], electron beam evaporation [20], sol–gel [21] soft chemical process [22], and spray pyrolysis [23]. Among all these methods, the spraying method is characterized as low cost, simple and suitable to produce large areas, with good purity for both metallic and non-metallic material deposition. Nickel (II) oxide adopts a sodium chloride structure, each unit cell has four formulas and octahedral Ni^{2+} and O_2 sites, Plane (111) is pure consists of Ni or O, while plane (100) is a mixed consisting of 50% nickel and 50% oxygen. The face (111) is a non-stable and polar face, while the face (100) is a stable and non-polar face. This kind of structure is known as a salt rock structure [23]. A literature review showed there are very few studies on the effect of low spray solution concentration on the characterization of NiO thin films deposited by spray pyrolysis for different applications. Reguig et al. 2006 [24] studied the impact of Nickel chloride precursor solution concentration of (0.05–0.5) M on the properties of NiO thin films deposited by spray pyrolysis method at a substrate temperature of 350 °C. They found that the thickness of the films increased from 0.5 μm to 3 μm as the solution concentration increased from below 0.3 M–0.5 M. Whereas the NiO films are of a p-type conductivity for the smaller molarity concentration and it becomes of a n-type conductivity for the higher molarity concentration. Hakkoum et al. 2020 [25] used different source solution quantities to deposit NiO thin films on a heated glass substrate at temperature of 350 °C and to modify their optical properties. They found that the transmittance and the energy gap decreased as the solution quantity increased as well as the film thickness was increased. Owoeye et al. 2023 [26] deposited NiO thin films using high purity nickel acetate precursors of various molarities from 0.1 M to 0.4 M on a glass substrate at a temperature of 350 °C. The XRD and EDX results confirmed the presence of Ni and O in the samples and by increasing the spray solution from 0.1 M to 0.4 M the thickness of the prepared films was increased from 43 nm to 49 nm and the quantity of Ni increased. Whereas the optical transmittance and optical energy gap were reduced as the solution molarity increased. This work aimed to deposit nickel oxide nano-structured thin films, and investigate the impact of molarity concentration of the spray solution on the crystal structure, surface morphology, and optical characterization of the prepared films for gas sensing application.

2. Experimental procedure

Nickel(II) oxide films were deposited by home-made spray pyrolysis method on 25 mm × 25 mm x 1 mm glass substrates. The substrates are previously cleaned using an Ultrasonic bath solution of ethanol, acetone, and deionized water for 15 min for each one.

Specified concentrations of Nickel (II) Nitrate Hexahydrate solution (0.01, 0.03, 0.05, 0.07, and 0.1) M were prepared, using the equation [27]:

$$M = \frac{W}{M_W} \times \frac{1000}{V} \quad (1)$$

where: M: is the solution molarity concentration, W, M_W: the weight and the molecular weight of Nickel salt, (M_W = 182.70 g/mol), V: distilled-water volume (100 ml), by dissolve (0.29079, 0.87238, 1.445397, 2.03555 and 2.9079) g of Nickel Nitrate in 100 ml of distilled water, with kept stirring for one hour. The substrate has been heated by a hotplate to keep the temperature at 420 ± 8 °C. To avoid the excessive substrate cooling of the film during the spraying processes the spraying process takes place in intervals each one continues 11 s and separates for two minutes. The rate of airflow was 5 ml/h and 30 cm is the distance between the spray nozzle and the substrate, which is sufficient to obtain uniform thin films. The thickness of the deposited films was measured using the weight method using the equation [28]:

$$t = \frac{\Delta m}{A.\rho} \quad (2)$$

where A is the surface area of the film and Δm (m_2-m_1) is the weight difference before m_1 and after m_2 deposition of Nickel oxide film and ρ is the density of NiO (6.67 g/cm^3). The thickness of the deposited films is about 250–350 nm. The weight method is the simplest method for film thickness determination and is most probably the determination of the mass gain of a coated substrate with an exact balance. It is possible to determine film

thickness using the weight method with sufficient accuracy for several practical applications.

The crystal structure and the lattice parameters of the deposited films were studied by X-ray diffraction using XPert Pro MPD diffractometer, Cu(kα) of 1.54059 Å wavelength. Maximum rated output 1.2 kW, a tube current of 30 mA, and Tube voltage 40 kV. The surface morphology and the surface topography of the prepared films were investigated using SEM analysis (Hitachi S-4160 SEM device) and AFM, model (TT-2 AFM Workshop, USA/SPM) respectively. Whereas the optical characteristics were studied using double-beam Maga-2100 UV-Vis spectrophotometer in the wavelength range (300–900) nm.

3. Results and discussion

3.1. Structural measurements

Most of the x-ray peaks confirm that the NiO films structure is of a polycrystalline nature, with good matching to the face-cantered cubic (FCC) phase, and the value of the lattice constant is a = 4.17382 Å. There are three peaks at diffraction angles of 38.51°, 44.73°, and 65.19° are shown in Fig. 1 belong to (111), (200) and (220) planes, respectively. These peaks are in good agreement with the information from International Centre for Diffraction Data (ICDD) card number (04–0835). Moreover, there are no additional peaks observed in the diffraction patterns of the prepared films which confirmed the purity of NiO cubic phase. The diffraction peaks intensity was increased as the spray solution molarity concentration increased; this can be attributed to the increase of NiO content and film thickness by increasing the spray solution concentration [24,25]. From XRD pattern of NiO film at 0.01 M spray solution concentration, there is a shift towards high angles which can be attributed to the low crystallinity of the film by the lower solution concentration which cusses a higher lattice strain and higher lattice constant as shown in Table 1. The crystallite size D values for the preferred orientation along (111) plane was calculated from the well-known Scherrer formula [29]:

$$D = \frac{0.9\lambda}{\beta \cos\theta} \tag{3}$$

where (β) is the full width at half maximum (FWHM) for a diffraction peak at an angle (θ) and λ = wavelength of the X-Ray beam.

Structural parameters including lattice constants (a), micro-strain (ϵ), interplanar spacing (d), and dislocation density (δ) of NiO thin films were calculated using the following equations [30–32], and the results are listed in Table 1.

$$n\lambda = 2d \sin\theta \tag{4}$$

$$d_{hkl} = \frac{a_{hkl}}{\sqrt{h^2 + k^2 + l^2}}. \tag{5}$$

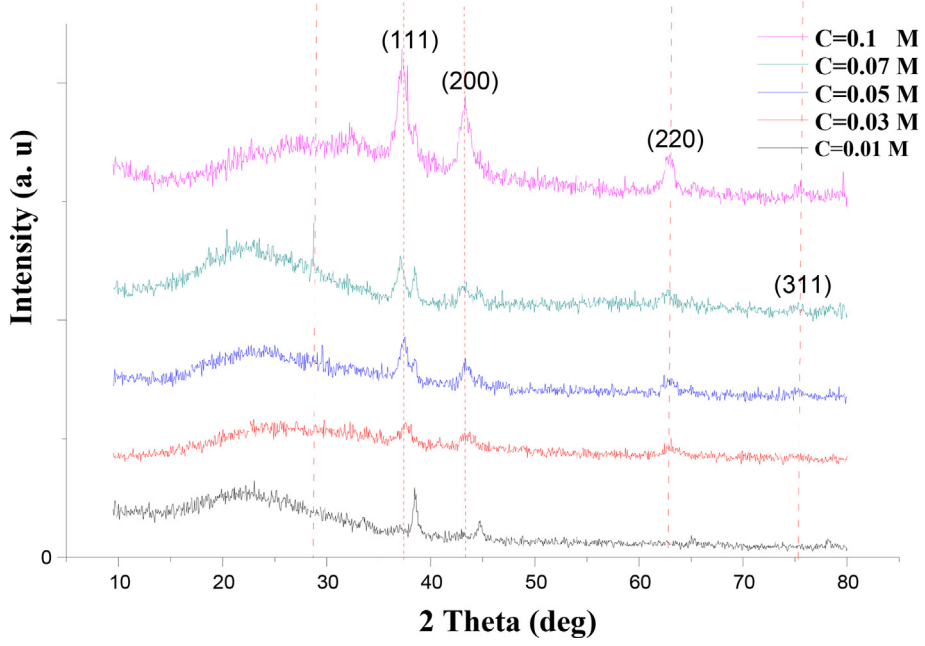

Fig. 1. XRD patterns of NiO thin films prepared at different precursor molarity.

Table 1. Structural parameters of NiO thin films at different spray solution molarity concentrations for the preferred orientation along (111) plane.

Precursor molarity (mol/L)	d (Å) exp.	a(Å) exp.	D(nm)	δ 10^{16} (lines/m^2)	ε (%)
0.01	2.33578	4.045	9.7834	104,38	−0.1461
0.03	2.38367	4.128	10.66988	87.83777	−0.1286
0.05	2.39681	4.151	12.18642	67.3361	−0.1238
0.07	2.33729	4.155	21.38948	21.85746	−0.1456
0.1	2.32914	4.163	28.53139	12.2844	−0.1485

$$\varepsilon = \frac{a_{\exp} - a_{bulk}}{a_{bulk}} \tag{6}$$

$$\delta = \frac{1}{D^2}\left(lines / m^2\right). \tag{7}$$

where n is diffraction order (n = 1), λ is the x-ray wavelength (1.5406 Å), θ is the diffraction angle, (hkl) is the Miller indices, a_{exp} and a_{bulk} is the lattice constant values experimentally obtained and standard JCPDS value respectively.

The values of lattice parameters for all films are less than the standard values (a = 4.17382 Å) of NiO. This difference in lattice parameter value can be attributed to the existence of impurities, defects, and internal strain, in the deposited films. These results are consistence with those of published studies [33,34]. Some structure parameters such as the micro-strain are directly dependence on the lattice constant c_{XRD} and the shift of its value from the standard value of JCPDS (c_{JCPDS}) (bulk) which can be evaluated using equation (6). It is worth mentioning that the negative sign strain expression denoted that the type of the micro-strain is a compressive strain. The average crystal sizes are directly proportional to solution concentration and the film crystallinity, which ranged from 9.7834 nm to 28.5314 nm. Also, it was noticed that the films which own the best structural properties are which the one that has the smallest mean strain value, which affects the degree of crystallinity as the film deposited using a higher molarity concentration (0.1 M) has the lower micro-strain and the higher crystallinity.

The morphological features have been studied by using SEM analysis, the SEM images (Fig. 2: a, b, c, d, and e) revealed that all NiO films have a homogeneous uniform distribution surface and nanocrystallites structure. The SEM micrographs show a homogenous distribution of grains that have different sizes which formed a smooth surface free of pinholes with the presence of some cracks as proof of good growth on the surface of the substrate. As the molarity concentration of the spray solution rises, no significant variation was observed, and the surface is smooth, and homogenous, with some cracks. The good adherent of the films to the substrate was observed which can be due to the pre-heated the substrate by using the spray pyrolysis method.

The overall elemental composition of the phases in the sample is calculated by using the energy dispersion of x-ray spectroscopy EDXS from the result of the SEM instrument as shown in Fig. 3(a, b, c and e), which confirm the existence of the elemental composition as shown in Table 2.

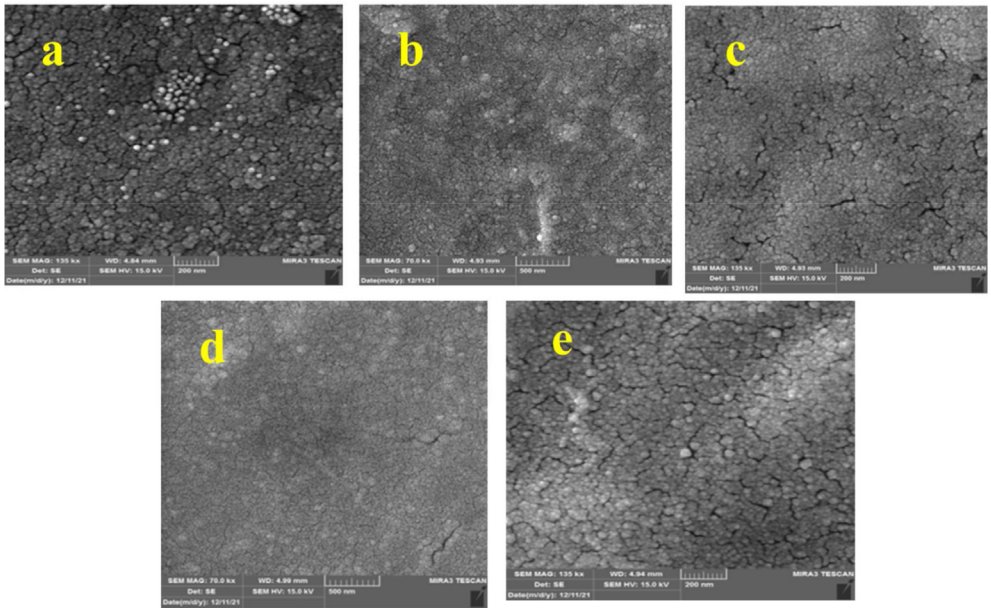

Fig. 2. SEM images of NiO nanostructure for varies concentrations(a: 0.01, b: 0.03,c: 0.05, d: 0.07, and e: 0.1) M.

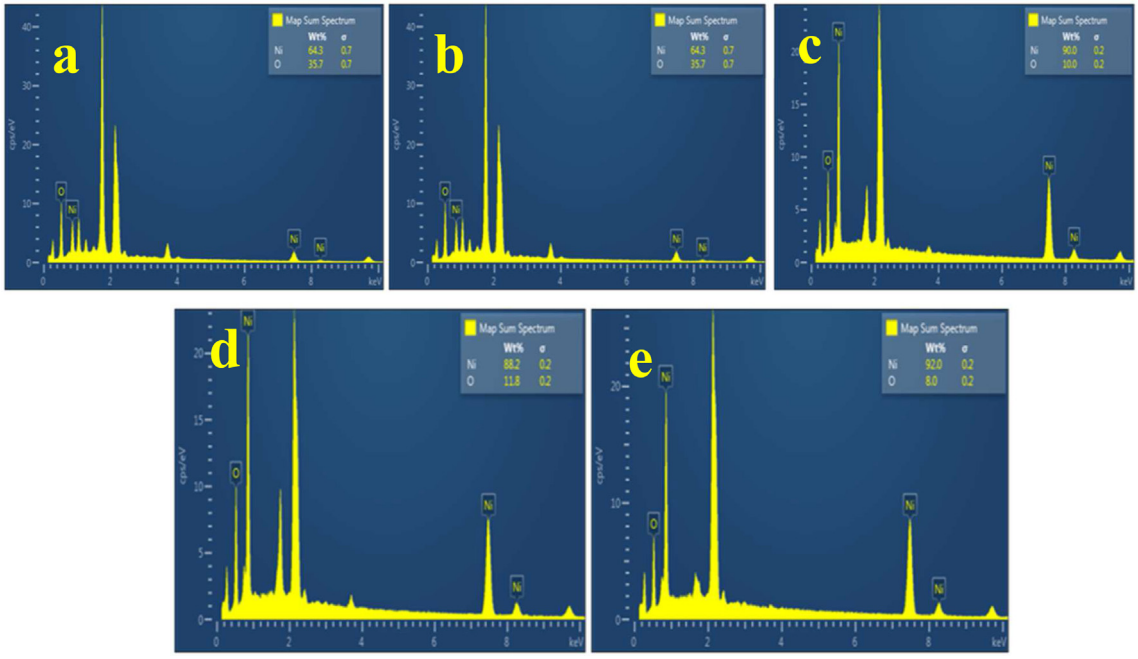

Fig. 3. EDX spectrum of NiO nanostructure for varies concentrations (a: 0.01, b: 0.03,c: 0.05, d: 0.07, and e: 0.1) M.

Table 2. EDX measurements of NiO nanostructure thin films at different concentrations

Element	0.01 M	0.03 M	0.05 M	0.07 M	0.1 M	Standard Label
O	35.66	12.97	9.95	11.85	8.01	SiO2
Ni	64.34	87.03	90.05	88.15	91.99	Ni
Total:	100.00	100.00	100.00	100.00	100.00	

The surface topographies of the deposited NiO films have been investigated using an Atomic force microscope (AFM). Fig. (4 a, b, c, d, and e) shows the AFM images of the NiO films spray deposited at different solution concentrations, which indicate that the surface topography is a nanostructure, and the RMS roughness for most films are lower than 15 nm. The AFM images showed homogeneous distribution of columnar grains and a direct proportion of the particle size to the concentration of the solution that was used to deposit them. The calculated values of grain size are ranged from 42.04 nm to 110.058 nm, the insets figures in Fig. 4 (a, b, c, d, and e) represent the grain size distribution for different spray solution concentrations. These results are consistent with XRD results and are listed in Table 3.

The compression between the variation of the crystallite size and the grain size values of NiO thin films deposited at different spray solution concentrations Table 3, it was found that both have the same behavior. The crystallite size and the grain size increase with the n crystallite size lower the than the values of the grain size which could be contains more crystallites [27,36].

3.2. Optical properties

The optical properties of deposited NiO thin films are studied by recording the transmittance spectra in the wavelength range of 300−900 nm. In the absorbance and transmittance spectra of the deposited NiO films, can be distinguished two regions Fig. 5 a and b; the higher than 350 nm, and the lower than 350 nm, the first region allowed an average transmittance between concentrations. This can be attributed to the increase of the thickness as well as the surface roughness of the deposited films by increasing the solution molarity and increase of NiO content [24,25] which obey the Beer−Lambert law [35]. The second region (lower than 350 nm) exhibits a decrease in the transparency for all samples. The highest value of the transmittance (over 80%) was obtained for the sample prepared at 0.01 M concentration.

The optical absorbance of NiO thin films Fig. 5 b shows strong absorption in the UV region at a wavelength of (300−380) nm and the absorbance was increased as the molarity concentration of the spray solution increased. Whereas the absorption edge was shifted towards long wavelengths and low energies (redshift) due to the introduction of localized states within the gap by increasing the density of states with the increase of the spray solution concentration [36−38]. The result was consistent whit those obtained by the literature [27,40,41]. It can be concluded that the prepared films can be

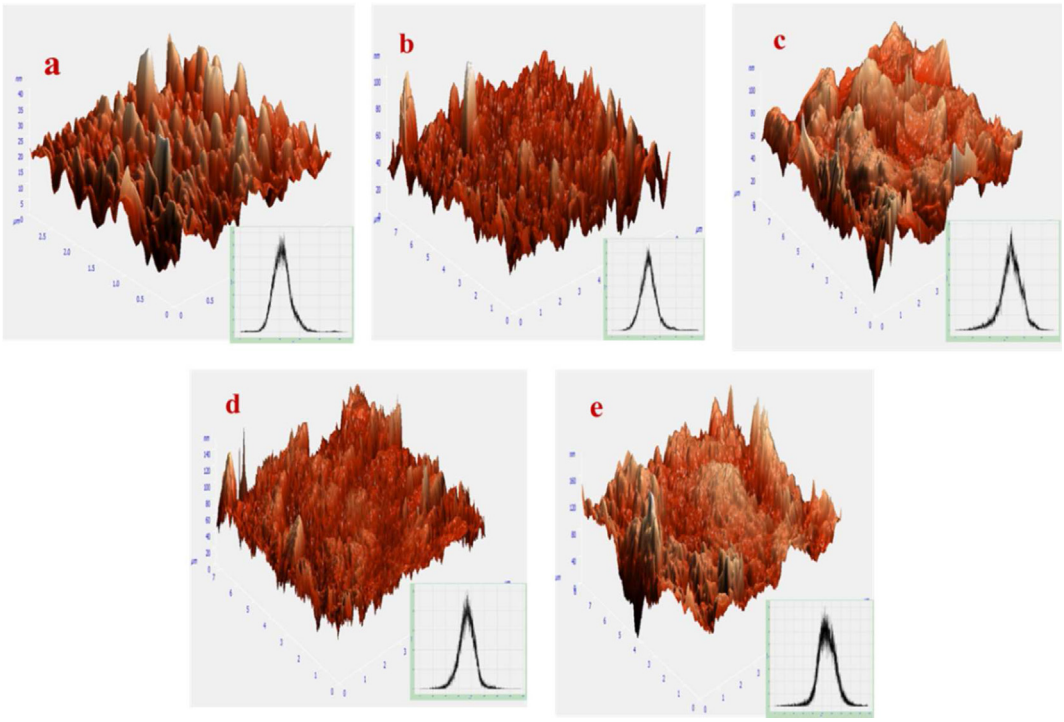

Fig. 4. 3D AFM images of NiO thin films deposited at different solution concentrations (a: 0.01, b: 0.03, c: 0.05, d: 0.07, and e: 0.1 M). Inset figures represent the grain size distribution for samples at different spray solution concentrations.

suitable for UV detectors and optoelectronic applications [39].

Fig. (6:a) shows a typical variation of $(\alpha h\nu)^2$ as a function of photon energy ($h\nu$) (Tauc equation) for all sprayed NiO thin films [35].

$$(\alpha h\nu) = B\left(h\nu - E_g\right)^{1/2} \tag{8}$$

The optical forbidden energy gap was estimated by extrapolating the linear part of the curve at $\alpha = 0$. The best linearity has been noticed in the former case. All curves characterize by a sharp absorption edge close to the band NiO gap. Table 4 contains the values of the band gaps. The direct optical band gaps (3.85 eV–3.15 eV) vs concentration graph shows that the band gaps are linear and inversely proportional to concentration. This inverse Proportional can be attributed to the compressive stress that results from the increase in the atoms in the lattice [37,39]. Also, gap decreasing with the increase of the solution quantity can be due to the rise of the film thickness or/and modification the films structure. Oxygen atoms coming up during the sprayed deposition which can replace either the interstitial site or substitution in the NiO lattice causes structural deformation (Ni vacancies or oxygen defects) [42,43]. These optical band gap results are in good an agreement with the results reported by [44–46]. Fig. (6:b) illustrates the relationship between $\ln\alpha$ vs. photon energy ($h\nu$) for all films, and the values of Urbach energy E_u have been calculated by the Urbach equation [35,36]:

$$\alpha = \alpha_o \exp\frac{h\nu}{E_u}. \tag{9}$$

Urbach energy was calculated from the slope of $\ln\alpha$ vs. photon energy ($h\nu$) graph, the results are tabulated in Table 4. The Utbach energy results indicate a linear increasing trend of whereas the band gap decrease, which means the defect states rise with increasing the solution molarity concentration. Urbach tails represent the width of available localized states within the optical band gap of NiO thin films, this localized states width is related directly to the exponential tail of the state's density near band edges [40].

Table 3. Average grain size, crystallite size and roughness of NiO thin films deposited at different solution concentration from AFM Images

Precursor molarity (mol/L)	Average grain size (nm)	Crystallite Size D(nm)	Average Roughness (nm)	Peak-to-peak (nm)
0.01	42.04	9.7834	6.98789	106.821
0.03	45.733	10.66988	7.61831	108.356
0.05	64.5739	12.18642	9.32	114.2
0.07	72.7976	21.38948	9.53234	155.459
0.1	110.058	28.53139	14.3348	195.672

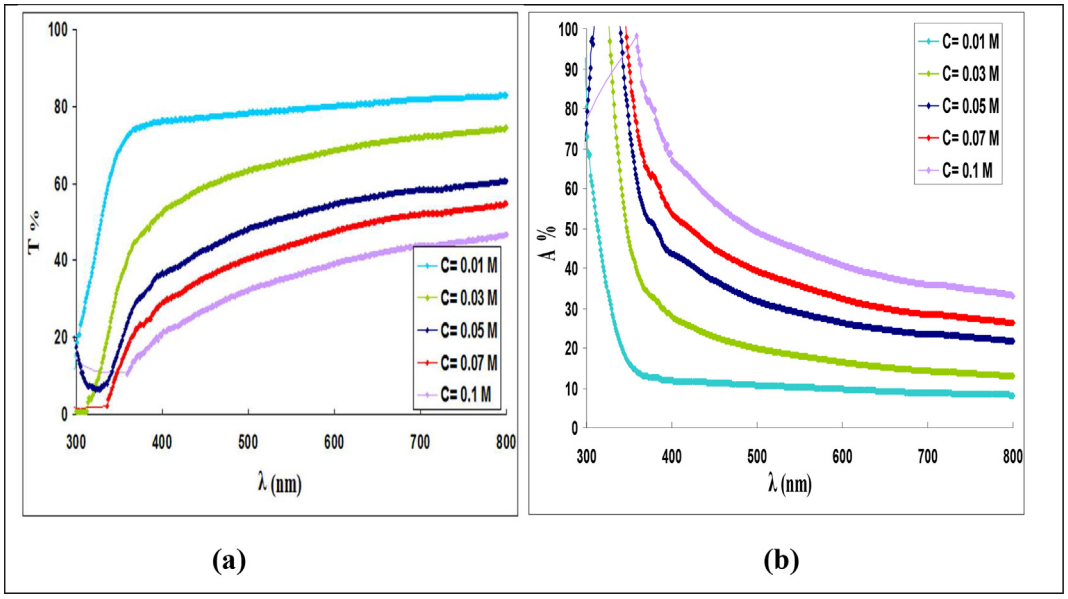

Fig. 5. a. Transmittance spectrum, b. Absorbance spectrum as a function of λ for NiO thin films at different concentration.

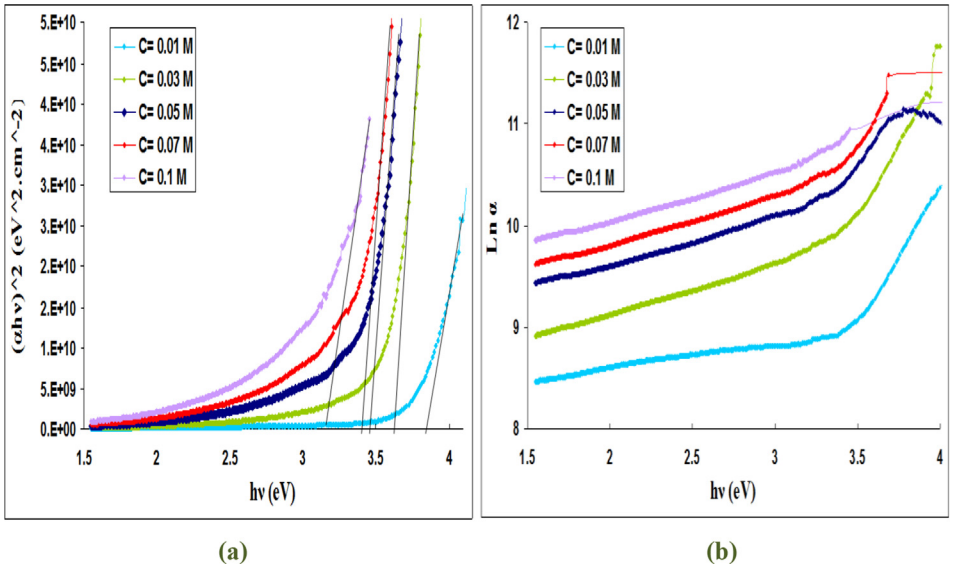

Fig. 6. Plot of a. $(\alpha h\nu)^2$, b. Ln(α) Vs. incident photon energy (hν) of NiO thin films at different precursor molarities concentrations.

Table 4. Optical parameters of NiO thin films at different precursor molarity concentration

Precursor molarity (mol/L)	E_g (eV)	Eu (eV)	T%
0.01	3.85	0.205	88
0.03	3.63	0.584	65
0.05	3.48	0.508	44
0.07	3.37	0.540	30
0.1	3.15	0.537	25

4. Conclusion

Nickel oxide thin films have been deposited on a glass substrate by the chemical spray pyrolysis method. The impact of spray solution molarity concentration on the structure, surface morphology, and optical characterization was investigated. The results showed that all deposited films have a polycrystalline structure of cubic phase and the

crystallinity and the crystallite size enhanced as the concentration rises. The surface morphology revealed a homogenous small granular structure and the surface roughness as well as the grain size were increased with the increase of the spray solution concentration. The optical characterization showed high transmittance and high absorbance in the Vis and UV regions respectively and the absorption edge was red shifting with the increment of the spray solution concentration. Therefore the energy band gap was decreased from 3.85 eV to 3.15 eV with an increment of the spray solution molarity concentration from 0.01 M to 0.1 M. We can be concluded that the electronic structure, surface topography, and the optical band gap can be controlled by the precursor concentration and the prepared NiO films are more suitable for optoelectronic, photovoltaics, and electrochromic applications.

References

[1] Jilani Asim, Mohamed Shaaban Abdel-Wahab, Ahmed Hosny Hammad. Advance deposition techniques for thin film and coating. Modern Technol Creat Thin-film Syst Coat 2017;2:137−49.

[2] Jeun Jeong-Hoon, Hong Seong-Hyeon. Porous SnO2 Films Fabricated by Anodic Oxidation and RIE Process and CuO Additives Effect on Gas Sensing Properties. Nanotechnology 2009;18:065707.

[3] Nur Amin Bitu Md, Islam Tanvir Nazmul, Islam Suravi, Uddin Farhad Syed Farid. Effect of substrate surface on the wide bandgap SnO2 thin films grown by spin coating. MRS Advances 2023;8:194−200. https://doi.org/10.1557/s43580-023-00515-3.

[4] Musa AMM, Farhad SFU, Gafur MA, Jamil ATMK. Effects properties of CuO thin films synthesized by dip-coating for CO_2 gas sensing. AIP Adv 2021;11:115004. https://doi.org/10.1063/5.0060471.

[5] Ghos Bijoy Chandra, Uddin Farhad Syed Farid, Majed Patwary Md Abdul, Majumder Shanta, Alauddin Hossain Md, Islam Tanvir Nazmul, Rahman Mohammad Atiqur, Tanaka Tooru, Guo Qixin. Influence of the Substrate, Process Conditions, and Postannealing Temperature on the Properties of ZnO Thin Films Grown by the Successive Ionic Layer Adsorption and Reaction Method. ACS Omega 2021;6(4):2665−74. https://doi.org/10.1021/acsomega.0c04837.

[6] Jao Meng-Huan, Cheng Chien-Chen, Lu Chun-Fu, Hsiao Kai-Chi, Su Wei-Fang. Low temperature and rapid formation of high quality metal oxide thin film via a hydroxide-assisted energy conservation strategy. J Mater Chem C 2018;6:9941−9. https://doi.org/10.1039/C8TC03544J.

[7] Palanichamya S, Raj Mohamedb J, Deva K, Kumarc, Satheesh Kumara PS, Pandiarajand S, Amalraj L. Physical properties of rare earth metal (Gd3+) doped SnO2 thin films prepared by simplified spray pyrolysis technique using nebulizer. Optik 2019;194:162887.

[8] Adel H. Omran Alkhayatt and Shymaa K. Hussian Fluorine highly doped nanocrystalline SnO2 thin films prepared by SPD technique. Mater Lett 2015;155:109−13.

[9] Yousif Salam Amir, Mohamed Abass Jenan. Structural, Morphological and Optical Characterization of SnO2: F thin films prepared by Chemical spray Pyrolysis. Int Lett Chem Phys Astron 2013;13:90−102.

[10] Boulila S, Ghamnia M, Boukhachem A, Ouhaibi A, Chakhoum MA, Fauquet C, Heresanu V, Tonneau D. Photocatalytical properties of NiO nanofilms doped with Ba. Phil Mag Lett 2020;110(6):283−93. https://doi.org/10.1080/09500839.2020.1760389.

[11] Angel Ezhilarasi A, Judith Vijaya J, Kaviyarasu K, John Kennedy L, Jothi Ramalingam R, Al-Lohedan Hamad A. Green synthesis of NiO nanoparticles using Aegle marmelos leaf extract for the evaluation of in-vitro cytotoxicity, antibacterial and photocatalytic properties. J Photochem Photobiol B Biol 2018;180:39−50.

[12] Likasari Icuk Dian, Astuti Rina Widi, Yahya Amri, Nur Isnaini, Purwiandono Gani, Hidayat Habibi, Wicaksono Wiyogo Prio. Is Fatimah, NiO nanoparticles synthesized by using Tagetes erecta L leaf extract and their activities for photocatalysis, electrochemical sensing, and antibacterial features. Chem Phys Lett 2021;780:138914.

[13] Zhao Y, Wang H, Wu C, Shi ZF, Gao FB, Li WC, et al. Structures, electrical and optical properties of nickel oxide films by radio frequency magnetron sputtering. Vacuum 2014;103:14−6.

[14] Soleimanpour AM, Jayatissaa AH, Sumanasekera G. Surface and gas sensing properties of nanocrystalline NiO thin films. Appl Surf Sci 2013;276:291−7.

[15] Gomaa MM, Sayed MH, Patil VL, Boshta M, Patil PS. Gas sensing performance of sprayed NiO thin films toward NO_2 gas. Journal of alloys and compound 2011;885:160908.

[16] Trabelsi ABG, Alkallas FH, Ziouche A, Boukhachem A, Ghamnia M, Elhouichet H. Structural defect impact on changing optical response and raising unpredicted ferromagnetic behaviour in (111) preferentially oriented nanocrystalline NiO films. Crystals 2022;12(5):692. https://doi.org/10.3390/cryst12050692.

[17] Guziewicz M, Klata P, Grochowski J, Golaszewska K, Kaminska E, Domagala JZ, et al. Hydrogen sensing properties of thin NiO films deposited by RF sputtering. Procedia Eng 2012;47:746−9.

[18] Ivan H, Jozef L, Helmut S, Peter V. properties of sputtered NiO thin films. J Electr Eng 2002;53(No.11−12):339−42.

[19] Jianga DY, Qina JM, Wangb X, Gaoa S, Lianga AC, Zhaoa JX. Optical properties of NiO thin films fabricated by electron beam evaporation. Vacuum 2012;86(8):1083−6.

[20] Romana CK, Peter B. Sol-Gel Prepared NiO Thin Films for Electrochromic pplications. Acta Chim Slov 2006;53:136−47.

[21] Allali Malika, Amine Dahamni Mohamed, Ghamnia Mostefa, Boukhachem Abdelwahab, Boukrédimi Djamel, Tonneau Didier, Fauquet Carole. Synthesis and Investigation of Pure and Cu-Doped NiO Nanofilms for Future Applications in Wastewater Treatment Rejected by Textile Industry Catalysts. 2022. p. 931. https://doi.org/10.3390/catal12090931. 12 (9).

[22] Ahmed JH. Study of optical and Electrical Properties of Nickel Oxide (NiO) Thin Films Deposited by Using a Spray Pyrolysis Technique. J Mod Phys 2014;5:2184−91.

[23] Benzscour H. Synthèse d'un oxyde transparent conducteur (OTC) par pulvérisation chimique (ZnO, NiO). MSc. Thesis, Badji Mokhtar University; 2008. Algeria.

[24] Reguig BA, Regragui M, Morsli M, Addou A Khelil M, Bernede JC. Effect of the precursor solution concentration on the NiO thin film properties deposited by spray pyrolysis. Sol Energy Mater Sol Cells 2006;90:1381−92. https://doi.org/10.1016/j.solmat.2005.10.003.

[25] Hakkoum Hadjer, Tibermacine Toufik, Sengouga Nouredine, Belahssen Okba, Ghougali Mebrouk, Benhaya Abdelhamid, Moumen Abderrahim, Comini Elisabetta. Effect of the source solution quantity on optical characteristics of ZnO and NiO thin films grown by spray pyrolysis for the design NiO/ZnO photodetectors. Opt Mater 2020;108:110434. https://doi.org/10.1016/j.optmat.2020.110434.

[26] Fathy Amany, Ahmed B, Ibrahim M, Abd Elkhalik S, Alexander Villinger, Abbas SM. Effect of precursor concentration on stoichiometry and optical properties of spray pyrolyzed nanostructured NiO thin film. Heliyon 2023;9:e13023. https://doi.org/10.1016/j.heliyon.2023.e13008.

[27] Aljarrah RM, Hamza HA. Effected of spraying solution concentration on SnO_2 films properties for photo-detector

application. In: AIP Conf Proc. 2457. AIP Publishing LLC; 2023. p. 1. 050011.
[28] Pearce R, Iakimov T, Andersson M, Hultman L, Spetz AL, Yakimova R. Epitaxially grown graphene based gas sensors for ultra sensitive NO2 detection. Sensors Actuators, B Chem. 2011;155(2):451−4552011.
[29] Williams G, Coles GSV. The Gas-Sensing Potential of Tin Dioxide Produced by a Laser Ablation Technique. MRS Bull 1999;24(6):25−9.
[30] Look David C, Reynolds DC, Litton CW, Jones RL, Eason DB, Cantwell G. Characterization of homoepitaxial p-type ZnO grown by molecular beam epitaxy. Applied Phys Lett 2002; 81(10):1830−2.
[31] Reddya AM, Reddyb AS, Reddya PS. Annealing effect on the physical properties of dc reactive magnetron sputtered nickel oxide thin films. Phys Proc 2013;49:9−14.
[32] Kelly PJ, Arnell RD. Magnetron sputtering: a review of recent developments and applications. Vacuum 2000;56:159−72.
[33] Leskelä M, Ritala M. Atomic layer deposition (ALD): from precursors to thin film structures. Thin Solid Films 2002; 409(1):138−46.
[34] Perednis D, Gauckler LJ. Thin film deposition using spray pyrolysis. J Electroceram 2005;14:103−11.
[35] Tauc J. Amorphous and liquid semiconductors. USA: Plenum Press; 1974.
[36] Adel H. Omran Alkhayatt, Structure, surface topography and optical characterization of Ag co − doped Cd1-xCuxO nanostructure thin films. J Kufa − Phys 2017;9(No.2):41−55.
[37] Benramache S, Benhaoua B. Influence of substrate temperature and Cobalt concentration on structural and optical properties of ZnO thin films prepared by Ultrasonic spray technique. Superlattice Microst 2012;52(4):807−15.
[38] Ukoba KO, Eloka-Eboka AC, Inambao FL. Review of nanostructured NiO thin film deposition using the spray pyrolysis technique. Renew Sustain Energy Rev 2018;82: 2900−15.
[39] Chtouki T, El Mrabet M, Goncharova A Tarbi, Erguig H. Comprehensive review of the morphological, linear and nonlinear optical characterization of spin-coated NiO thin films for optoelectronic applications. Opt Mater 2021;118: 111294.
[40] Aftab Muzamil, Butt MZ, Ali Dilawar, Bashir Farooq, Khan Taj Muhammad. Optical and electrical properties of NiO and Cu-doped NiO thin films synthesized by spray pyrolysis. Opt Mater 2021;119:111369.
[41] Li X, Zhang X, Li Z, Qian Y. Synthesis and characteristics of NiO nanoparticles by thermal decomposition of nickel dimethylglyoximate rods. Solid State Commun 2006;137: 581−4.
[42] Ali D, Butt MZ, Arif B, Al-Ghamdi AA, Yakuphanoglu F. The role of Al, Ba, and Cd dopant elements in tailoring the properties of c-axis oriented ZnO thin films. Phys B Condens Matter 2017;506:83−93.
[43] Sharma Ratnesh, Acharya AD, Shrivastavaa SB, Patidarc Manju Mishr, Gangrade Mohan, Shripathi T, Ganesan V. Studies on the structure optical and electrical propertiesof Zn-doped NiO thin films grown by spray pyrolysis. Optik 2016;127:4661−8.
[44] Sharma S, Periasamy C, Chakrabarti P. Thickness dependent study of RF sputtered ZnO thin films for optoelectronic device applications. Electron Mater Lett 2015;11(6):1093−101.
[45] Desai JD, Min S-K, Jung K-D, Joo andO-S. Spray pyrolytic synthesis of large area NiOx thin films from aqueous nickel acetate solutions. Appl Surf Sci 2006;253(4):1781−6.
[46] Juybari HA, Bagheri-Mohagheghi M-M, Shokooh-Saremi M. Nickel-lithium oxide alloy transparent conducting films deposited by spray pyrolysis technique. J Alloys Compd 2011;509(6):2770−5.